OPEN

Citation: Cell Death and Disease (2014) 5, e1311; doi:10.1038/cddis.2014.275

www.nature.com/cddis

Ketamine alters cortical integration of GABAergic interneurons and induces long-term sex-dependent impairments in transgenic Gad67-GFP mice

C Aligny[1], C Roux[1], N Dourmap[1], Y Ramdani[1], J-C Do-Rego[2], S Jégou[1], P Leroux[1], I Leroux-Nicollet[1], S Marret[1,3] and BJ Gonzalez*[,1]

Ketamine, a non-competitive N-methyl-D-aspartate (NMDA) antagonist, widely used as an anesthetic in neonatal pediatrics, is also an illicit drug named Super K or KitKat consumed by teens and young adults. In the immature brain, despite several studies indicating that NMDA antagonists are neuroprotective against excitotoxic injuries, there is more and more evidence indicating that these molecules exert a deleterious effect by suppressing a trophic function of glutamate. In the present study, we show using Gad67-GFP mice that prenatal exposure to ketamine during a time-window in which GABAergic precursors are migrating results in (i) strong apoptotic death in the ganglionic eminences and along the migratory routes of GABAergic interneurons; (ii) long-term deficits in interneuron density, dendrite numbers and spine morphology; (iii) a sex-dependent deregulation of γ-aminobutyric acid (GABA) levels and GABA transporter expression; (iv) sex-dependent changes in the response to glutamate-induced calcium mobilization; and (v) the long-term sex-dependent behavioral impairment of locomotor activity. In conclusion, using a preclinical approach, the present study shows that ketamine exposure during cortical maturation durably affects the integration of GABAergic interneurons by reducing their survival and differentiation. The resulting molecular, morphological and functional modifications are associated with sex-specific behavioral deficits in adults. In light of the present data, it appears that in humans, ketamine could be deleterious for the development of the brain of preterm neonates and fetuses of addicted pregnant women.
Cell Death and Disease (2014) **5,** e1311; doi:10.1038/cddis.2014.275; published online 3 July 2014

Neonatal brain lesions, which affect both preterm and term infants, result in cerebral palsy and cognitive deficits.[1] The main risks associated with these lesions are prematurity, hypoxia-ischemia, hemorrhages, fetal-placental infections and exposure to toxins.[1,2] Although the underlying neurochemical processes are complex and only partially elucidated, the production of pro-inflammatory cytokines, free-radical stress induced by both reactive oxygen and nitrogen species, and the massive release of glutamate at both synaptic and extrasynaptic sites, leading to an excitotoxic cell death, have been described.[3,4] In particular, because of its high permeability to calcium, the N-methyl-D-aspartate (NMDA) receptor has been shown to have a key role in excitotoxicity, and several studies reported that NMDA receptor antagonists exert a protective effect in both adults and neonates.[4–6] However, the innocuousness of NMDA antagonists in the developing brain is debatable. Indeed, several research groups have described a deleterious effect of molecules such as MK801 or memantine in the immature neocortex.[4,7–9] In particular, it has been shown that MK801 exerts a dual effect in cultured cortical slices from mouse neonates; although it reduces excitotoxic death in the deep cortical layers V and VI, it has a pro-apoptotic effect on immature GABAergic interneurons present in the superficial layers II–IV.[7]

Because of its short onset of action, rapid clearance and low influence on respiratory and cardiac functions, ketamine is an anesthetic widely used in neonatal pediatrics.[10,11] However, similar to MK801, ketamine is a non-competitive NMDA-receptor blocker, and even though its effects are less long-lasting than those of MK801, recent studies point to neurotoxic effects of ketamine in the immature brain of rats and non-human primates.[12,13] These reports raise the possibility that ketamine could also have deleterious effects in the developing human brain.[14] Moreover, ketamine is also listed as an illicit drug (named Special K, KitKat or Super K) in most countries and is increasingly used by teens and young adults at raves, with the associated risk of addiction and consumption during pregnancy.[15,16] It appears, therefore, that the clinical use of ketamine in pediatrics as well as drug-abuse practices lead to a risk of perinatal exposure during a time-window in which GABAergic interneurons are still differentiating.[17]

[1]ERI28, NeoVasc, Laboratory of Microvascular Endothelium and Neonatal Brain Lesions, Institute of Research for Innovation in Biomedicine, Normandy University, Rouen, France; [2]Behavioural Analysis Facility, Institute of Research for Innovation in Biomedicine, Normandy University, Rouen, France and [3]Department of Neonatal Paediatrics and Intensive Care, Rouen University Hospital, Rouen, France

*Corresponding author: BJ Gonzalez, ERI28 NeoVasc, Laboratory of Microvascular Endothelium and Neonatal Brain Lesions, Institute of Research for Innovation in Biomedicine, Normandy University, Rouen 76183, France. Tel: +33 2 35148547; Fax: +33 2 35148356; E-mail: bruno.gonzales@univ-rouen.fr

Abbreviations: aCSF, artificial cerebrospinal fluid; DMEM, Dulbecco's modified Eagle's medium; E15, embryonic day 15; GABA, γ-aminobutyric acid; GAD, glutamic acid decarboxylase; GAT1–3, GABA transporter 1–3; MGE, median ganglionic eminence; GD15, gestational day 15; GFP, green fluorescence protein; HPLC, high-performance liquid chromatography; MAGUK, membrane-associated guanylate kinase; NMDA, N-methyl-D-aspartate; PBS, phosphate buffer saline; PSD95, post-synaptic density protein 95; ROI, region of interest

Received 20.2.14; revised 16.5.14; accepted 23.5.14; Edited by D Bano

Based on our recent demonstration that MK801 affects the survival of GABAergic interneurons, we hypothesized that ketamine would also interfere with the GABAergic system and result in long-term deficits. Here we tested this hypothesis by using Gad67-GFP transgenic mice to investigate *ex vivo* and *in vivo* the effects of prenatal exposure to ketamine on (i) the survival of GABAergic precursors, (ii) the molecular and morphometric characteristics of GABAergic interneuron differentiation, (iii) glutamate-induced neuronal activation and (iv) the long-term impairment of motor activity.

Results

Effects of ketamine on the apoptotic death of precursors from cultured E15 GEs. Several parameters, that is, caspase-3 activity, caspase-3 cleavage, BAX expression and mitochondrial integrity were used to investigate the effects of ketamine on apoptotic death in embryonic day 15 (E15) ganglionic eminences (GEs) (Figure 1). Although a 6-h exposure of E15 GEs to ketamine (100 μM) had no effect on caspase-3 activity, a significant increase was detected after 24 h (**$P=0.0039$, $n=10$; Figure 1a). A pilot experiment in which embryos were sexed showed no difference between females and males with respect to the effect of ketamine on caspase-3 activity (Supplementary Figure 1). Western blotting studies revealed a significant increase in caspase-3 cleavage (*$P=0.0286$, $n=4$) after a 24-h exposure to ketamine (100 μM; Figure 1b). Immunohistochemistry indicated that cleaved caspase-3-positive cells were mainly localized in the median and lateral ganglionic eminence (M/L GE), while low labeling was found in the developing striatum (Str; Figures 1c–f). Similarly, a significant increase in BAX expression levels was seen after 24 h (*$P=0.0290$, $n=4$; Figure 1g). BAX-immunoreactive cells were preferentially localized in the premigratory zone of the MGE (Figures 1h and i). The use of the ratiometric probe JC-1 showed that ketamine (100 μM) significantly compromised mitochondrial integrity (**$P=0.0084$, $n=16$) in E15 GEs after 12 h of treatment (Figures 1j–l).

Effects of ketamine on the apoptotic death of GABAergic precursors in the developing cortex at E15. Western blotting studies using several markers of the GABAergic lineage – Nkx2.1, DlX1 and LHX6 – showed that ketamine (100 μM) induced a significant decrease in protein levels (*$P=0.0411$, $n=6$; *$P=0.0379$, $n=7$; *$P=0.0152$, $n=6$, respectively) whatever the marker considered (Figures 2a–c). Histological analysis of cleaved caspase-3-positive cells after exposure to ketamine (100 μM) revealed that in addition to the GEs, immunoreactive cells were also localized along the migratory routes of GABAergic precursors (Figure 2d).[18] In particular, double immunohistochemistry experiments revealed that the Nkx2.1-immunoreactive region overlapped with that of cleaved caspase-3 (Figures 2e and f). At higher magnifications, numerous Nkx2.1-positive cells were also positive for cleaved caspase-3 after ketamine treatment (100 μM; Figures 2g and h). High-magnification acquisitions were done in the cortical regions where Nkx2.1 was expressed (Figure 2i) and cell quantification by image analysis revealed that ketamine (100 μM) significantly increased the proportion of Nkx2.1$^+$-cleaved caspase-3$^+$ co-labeled cells (**$P=0.0022$, $n=6$; Figure 2j).

Long-term effects of prenatal exposure to ketamine on morphometric characteristics of Gad67-GFP interneurons in cortical layers II–IV. For *in vivo* experiments, pregnant females received daily injections of ketamine (50 mg/kg) from gestational day 15 (GD15) to GD20 in order to induce analgesia for 3 h. The density of Gad67-GFP cells was quantified 45 days after birth. This population of interneurons was observed in cortical layers II–IV (Figures 3a and b). When the sex of the animals was not taken into consideration, prenatal exposure to ketamine induced a significant decrease in Gad67-GFP cell density (****$P<0.0001$, $n=16$ (females + males); Figure 3c). When sex was considered, the effect of ketamine on Gad67-GFP cell density affected both males (***$P=0.0003$, $n=8$) and females (*$P=0.0379$, $n=8$; Figure 3c). In addition, 3D reconstructions were used to quantify the number of primary neurites in Gad67-GFP cells (Figure 3d). Prenatal exposure to ketamine reduced the number of primary neurites in males (*$P=0.0159$, $n=5$) and females (*$P=0.0317$, $n=5$; Figure 3e). The quantification by western blotting of green fluorescence protein (GFP) levels revealed a significant reduction in males (**$P=0.0079$, $n=5$) and females (**$P=0.0079$, $n=5$) exposed *in utero* to ketamine (Figure 3f). In the same way, a decrease of cortical Gad levels was retrieved in males (**$P=0.0079$, $n=5$) and females (**$P=0.0079$, $n=5$) exposed to ketamine (Figure 3g). In order to investigate the effect of ketamine on the entire population of GABAergic neurons, γ-aminobutyric acid (GABA) immunohistochemistry experiments were done on Gad67-GFP mice (Supplementary Figure 2). In the superficial cortical layers II–IV, ketamine (50 mg/kg) induced a decrease of the density of GABAergic interneurons in both males and females (**$P=0.0028$, $n=8$ and ***$P=0.0006$, $n=8$, respectively), while no effect was seen in cortical layers V–VI (Supplementary Figure 2). As dendritic spines are indicative of cell differentiation, we quantified their densities and morphologic subtypes in Gad67-GFP neurons exposed or not to ketamine during prenatal life (Figures 4a–d). 3D reconstructions of *Z*-stack confocal acquisitions showed that prenatal exposure to ketamine induced a significant reduction in spine density in both males and females (*$P=0.0200$, $n=40$ and *$P=0.0222$, $n=40$, respectively; Figures 4a–c). This effect was also associated with the altered distribution of filopodia, stubby and mushroom subtypes of spines (**$P=0.0089$, χ^2-test $=9.445$; Figure 4d).

Effects of prenatal exposure to ketamine on GABA and GABA transporter levels. GABA is the main inhibitory neurotransmitter of the central nervous system. After its release, GABA is removed from the synaptic cleft or extrasynaptic space by transporters of the GABA transporter (GAT) family. One of these, GAT-1, is mostly localized in neurons including Gad67-GFP neurons (Figure 5a), while another, GAT-3, is mainly detected in glial processes (Figure 5b). Western blotting experiments showed a significant increase in GAT-1 (*$P=0.0317$, $n=5$) and GAT-3

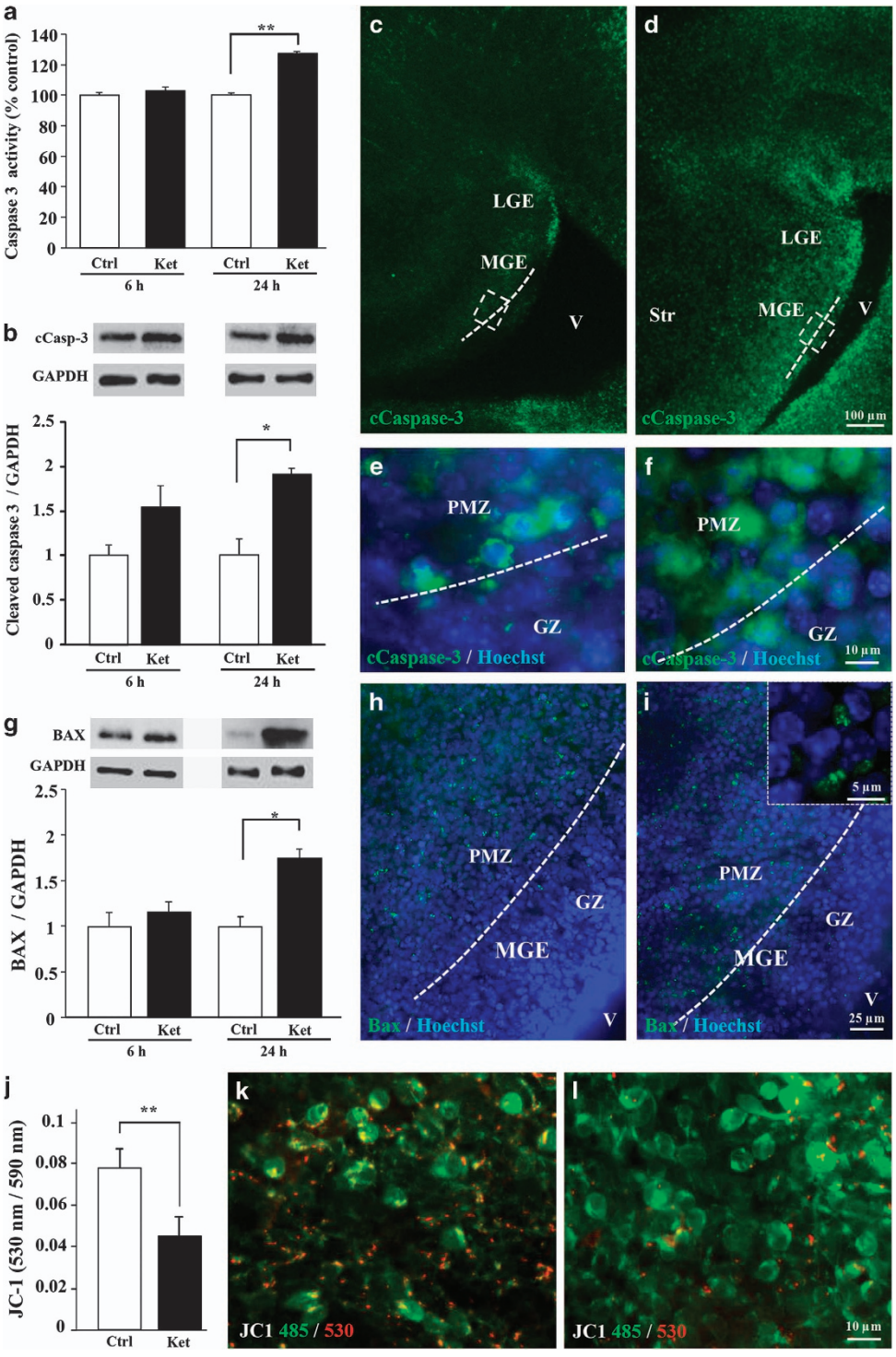

Figure 1 Effect of ketamine on induction of apoptosis in E15 GE. (**a**) Quantification of caspase-3 activity in cultured E15 GEs after 6 and 24 h of exposure to ketamine (100 μM). (**b**) Quantification by western blotting of the effect of ketamine (100 μM) on caspase-3 cleavage after 6 and 24 h of exposure. Visualization at low (**c** and **d**) and high magnifications (**e** and **f**; insets) of cleaved caspase-3-positive cells in a control E15 GE (**c** and **e**) and after a 24-h exposure to ketamine (100 μM; **d** and **f**). GZ, germinative zone; PMZ, premigratory zone; Str, striatum; V, ventricle. (**g**) Quantification by western blotting of BAX levels in cultured E15 GEs after 6 and 2 h of ketamine treatment (100 μM). Visualization of BAX immunoreactivity in a control E15 GE (**h**) and after a 24-h exposure to ketamine (100 μM; **i**). Note that immunolabeling is preferentially localized in the PMZ and not the GZ of the GE. Inset: BAX labeling at high magnification. (**j**) Quantification of the fluorescent signals (590 nm/530 nm) emitted by the JC-1 probe after a 12-h treatment of the E15 GE with ketamine (100 μM). Visualization of the mitochondrial (orange) and cytosolic (green) forms of JC-1 in a control E15 GE (**k**) and after a 12-h exposure to ketamine (100 μM; **l**). Each value represents the means ($\pm$ S.E.M.) of at least four independent experiments. *$P<0.05$; **$P<0.01$ for ketamine *versus* control groups, Mann–Whitney *U*-test and Wilcoxon signed-rank test

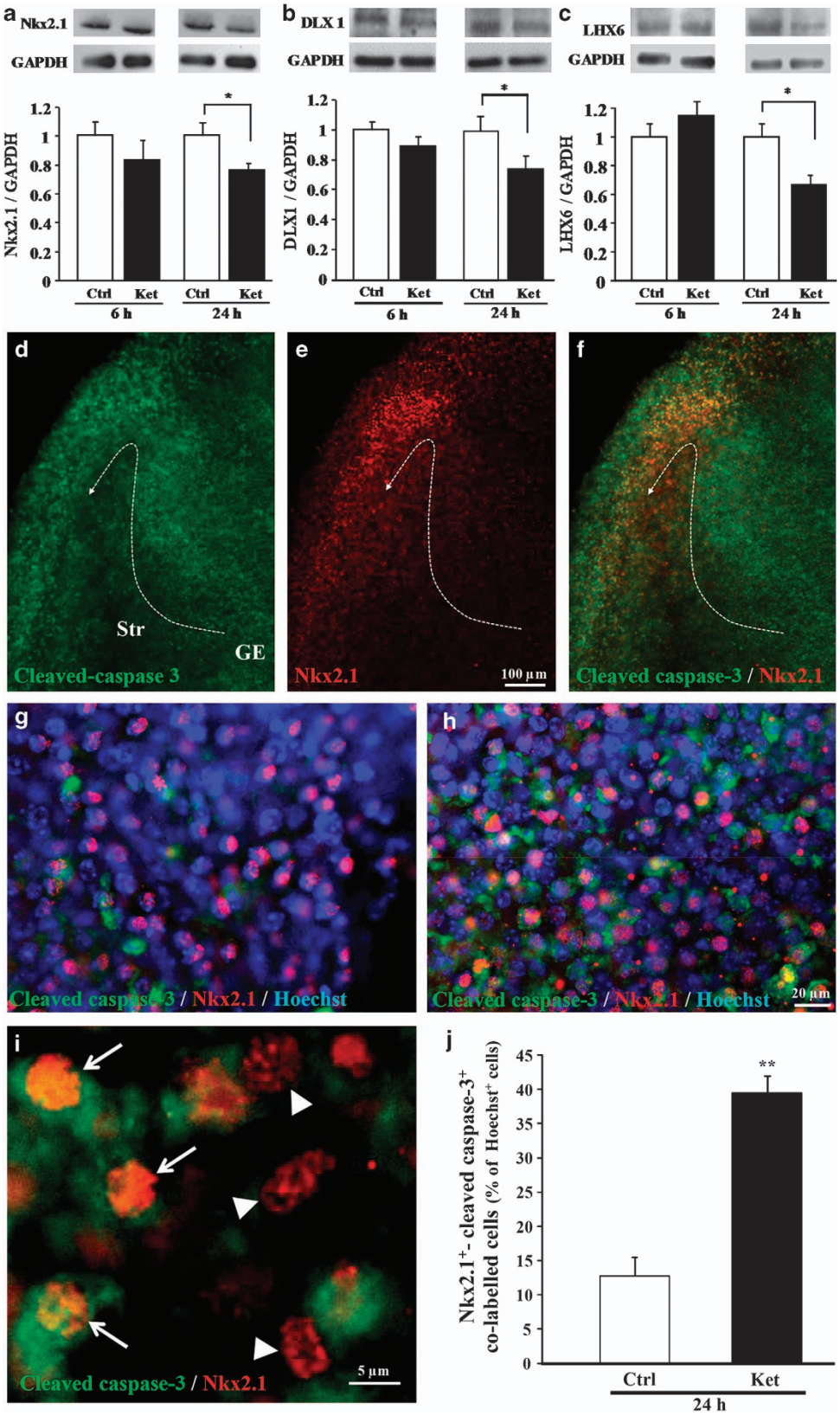
a
Nkx2.1
GAPDH
Nkx2.1 / GAPDH
b
DLX1
GAPDH
DLX1 / GAPDH
c
LHX6
GAPDH
LHX6 / GAPDH
Ctrl
Ket
6 h
24 h
d
Str
GE
Cleaved-caspase 3
e
Nkx2.1
100 µm
f
Cleaved caspase-3 / Nkx2.1
g
Cleaved caspase-3 / Nkx2.1 / Hoechst
h
Cleaved caspase-3 / Nkx2.1 / Hoechst
20 µm
i
Cleaved caspase-3 / Nkx2.1
5 µm
j
Nkx2.1+- cleaved caspase-3+ co-labelled cells (% of Hoechst+ cells)
24 h

(**$P=0.0079$, $n=5$) expression levels in postnatal day 45 (P45) males previously exposed to ketamine *in utero*, while no effect was seen in females (Figures 5c and d). Synaptophysin, a synaptic vesicle glycoprotein, was also quantified, but no difference in its levels was seen in any group (Supplementary Figure 2). Cortical GABA concentrations were quantified by high-performance liquid chromatography (HPLC; Figures 5e and f). The peak

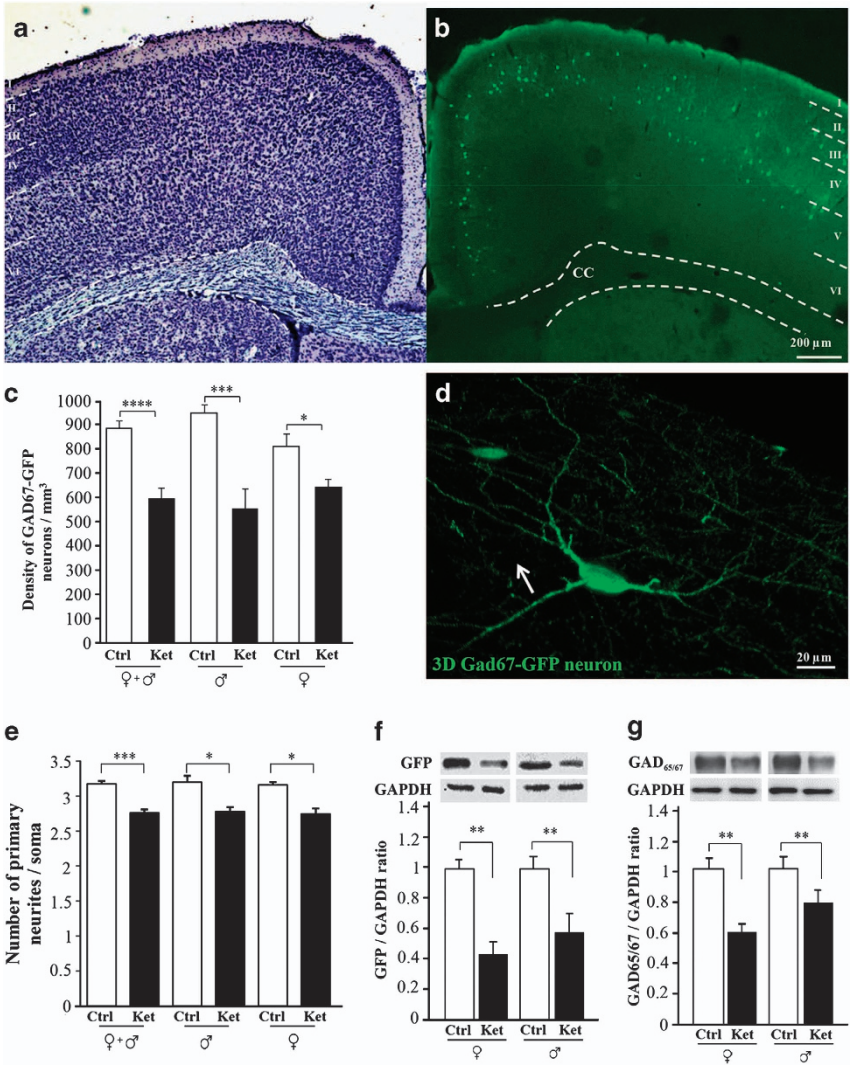

Figure 3 Long-term effect of *in vivo* prenatal exposure to ketamine on the density of Gad67-GFP cells in the superficial cortical layers II–IV. Cresyl violet staining revealing the different cortical layers in P45 mice (**a**) and the preferential localization of Gad67-GFP cells in layers II–IV (**b**). (**c**) Quantification of the effect of prenatal ketamine exposure on the density of Gad67-GFP neurons in layers II–IV of female and male P45 mice. (**d**) 3D reconstruction of a Gad67-GFP cell from the neocortex of a P45 mouse. Arrow indicates a primary neurite. (**e**) Quantification of the effect of prenatal exposure to ketamine on the number of primary neurites in Gad67-GFP interneurons in layers II–IV of female and male P45 mice. (**f**) Quantification by western blotting of the effect of prenatal exposure to ketamine on GFP levels in female and male P45 mice. **(g)** Quantification by western blotting of the effect of prenatal exposure to ketamine on Gad levels in female and male P45 mice. For western blotting experiments, each value represents the mean (±S.E.M.) of five independent experiments. For morphometric analyses, each value represents the mean (±S.E.M.) of at least five animals per group. *$P<0.05$; **$P<0.01$; ***$P<0.001$; ****$P<0.0001$ for ketamine *versus* control groups, Mann–Whitney *U*-test

Figure 2 Effect of ketamine on protein levels of the GABAergic lineage markers Nkx2.1, DLX1 and LHX6. Quantification by western blotting of Nkx2.1 (**a**), DLX1 (**b**) and LHX6 (**c**) levels in cultured E15 GEs after 6 and 24 h of ketamine treatment (100 μM). Double labeling of cleaved caspase-3- (**d**) and Nkx2.1-positive cells (**e**) in the developing cortex of E15 brain slices after a 24-h treatment with ketamine (100 μM). Note that Nkx2.1 labeling partially overlaps with the cleaved caspase-3 signal (**f**), which is preferentially localized in the previously characterized migratory routes of GABAergic precursors (dashed arrow). Visualization of cleaved caspase-3 and Nkx2.1 double-labeled cells in the developing cortex from control (**g**) and ketamine-treated (**h**) E15 slices. Note the strong co-localization of the two signals after ketamine exposure. The total number of nuclei was visualized by Hoechst labeling. (**i**) High magnification confocal acquisition visualizing Nkx2.1 cells immunopositive (arrows) or immunonegative (arrow heads) for the cleaved caspase-3. **(j)** Quantification of the effect of a 24 h (100 μM) ketamine exposure on Nkx2.1/cleaved caspase-3 immunoreactive cells. For western blot studies, each value represents the mean (±S.E.M.) of at least six independent experiments. For cell quantification, each value represents the mean (±S.E.M.) of 18 ROI from 6 different slices. *$P<0.05$; **$P<0.01$ for ketamine *versus* control groups, Mann–Whitney *U*-test

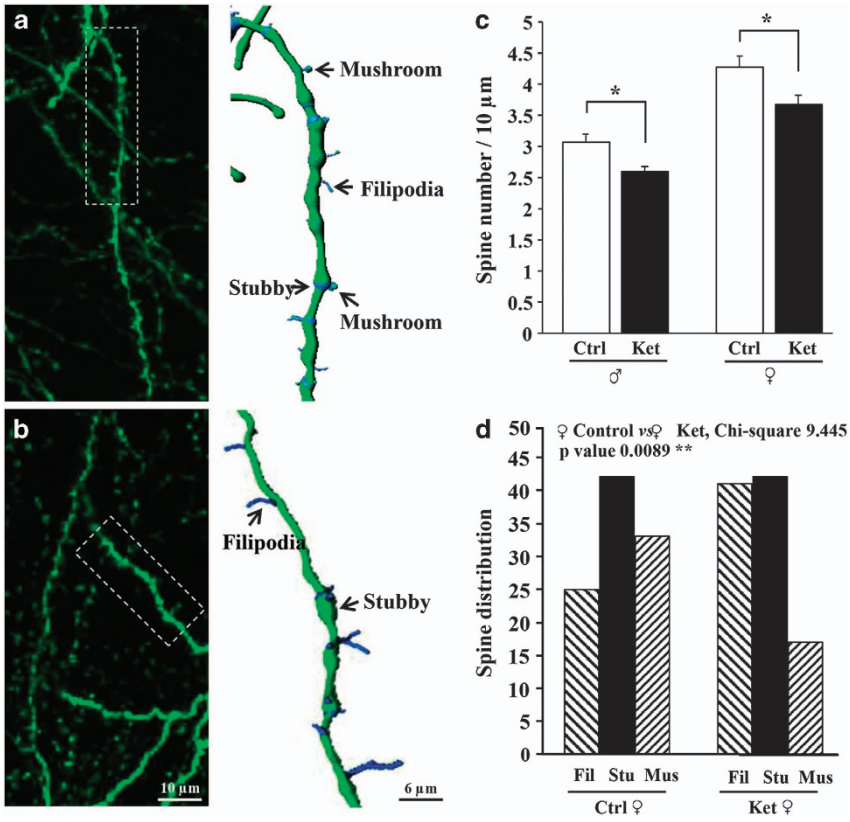

Figure 4 Long-term effect of *in vivo* prenatal exposure to ketamine on dendritic spines of Gad67-GFP neurons in cortical layers II–IV. Confocal microscopic photographs (left panels) showing dendritic spines in Gad67-GFP interneurons from control (**a**) and ketamine-treated (**b**) mice. Dashed rectangles illustrate dendrites used for 3D reconstruction and spine characterization (right panels). (**c**) Quantification of spine density on dendrites from Gad67-GFP interneurons in cortical layers II–IV of female and male P45 mice. Each value represents the mean (± S.E.M.) of 40 dendrites (10 dendrites analyzed per animal). $^{*}P<0.05$ for ketamine *versus* control groups, Mann–Whitney *U*-test. (**d**) Distribution of the different spine morphologies on dendrites from Gad67-GFP interneurons in layers II–IV of female P45 mice; χ^2-analysis of spine-type distribution obtained from quantification of three slices per animals and three animals per group

representing GABA eluted at 35.3 min (Figure 5e). At P45, the mean concentration of GABA in males from the control group was $0.11 \pm 0.02\,\mu$M/mg (Figure 5f). Concentrations were significantly increased in males from the ketamine group ($^{**}P=0.0022$, $n=6$; Figure 5f). No difference in cortical GABA levels was found between females from the control and ketamine groups (Figure 5f).

Effects of prenatal exposure to ketamine on glutamate-induced neuronal activity. As neuronal activity is controlled by the fine tuning between inhibitory and excitatory neurotransmission, we investigated the impact of prenatal ketamine exposure on glutamate-induced intracellular calcium mobilization, an index of neuronal activity (Figure 6). Calcimetry experiments using the ratiometric calcium probe Fura-2 were performed on P15 brain slices (Figure 6a). In both females and males from the control group, glutamate (400 μM) induced an increase in intracellular calcium levels in cortical cells (Figures 6a–c). For both sexes, the glutamate-induced calcium increase was delayed in animals exposed *in utero* to ketamine (Figures 6b and c). In addition, the amplitude of the calcium increase was markedly exacerbated ($^{**}P=0.0019$, $n=16$) in females exposed *in utero* to ketamine (Figures 6c and d). The quantification of the GluN1 NMDA receptor subunit showed that ketamine exposure during prenatal life reduced GluN1 protein levels in both males and females ($^{*}P=0.0286$, $n=4$; Figure 6e). However, the expression of post-synaptic density protein 95 (PSD95), a MAGUK (membrane-associated guanylate kinase) protein involved in the regulation of excitatory synapses, was differently regulated between males and females, decreased in males ($^{**}P=0.0022$, $n=6$) but significantly increased in females exposed to ketamine ($^{**}P=0.0087$, $n=6$; Figure 7a). Confocal microscopy acquisitions showed that even if not exclusively, PSD95 immunoreactivity overlapped with Gad67-GFP soma and dendrites (Figures 7b–d). At high magnification, several PSD95-immunoreactive puncta were closely associated with subtypes of Gad67-GFP dendritic spines (Figures 7e–g). Moreover, the quantification of cortical glutamate levels at P45 revealed a slight but no significant increase in animals exposed *in utero* to ketamine (Supplementary Figure 3).

Long-term effects of prenatal exposure to ketamine on locomotor activity. The histological, molecular and functional experiments above have revealed that prenatal exposure to ketamine induces alterations of the cortical

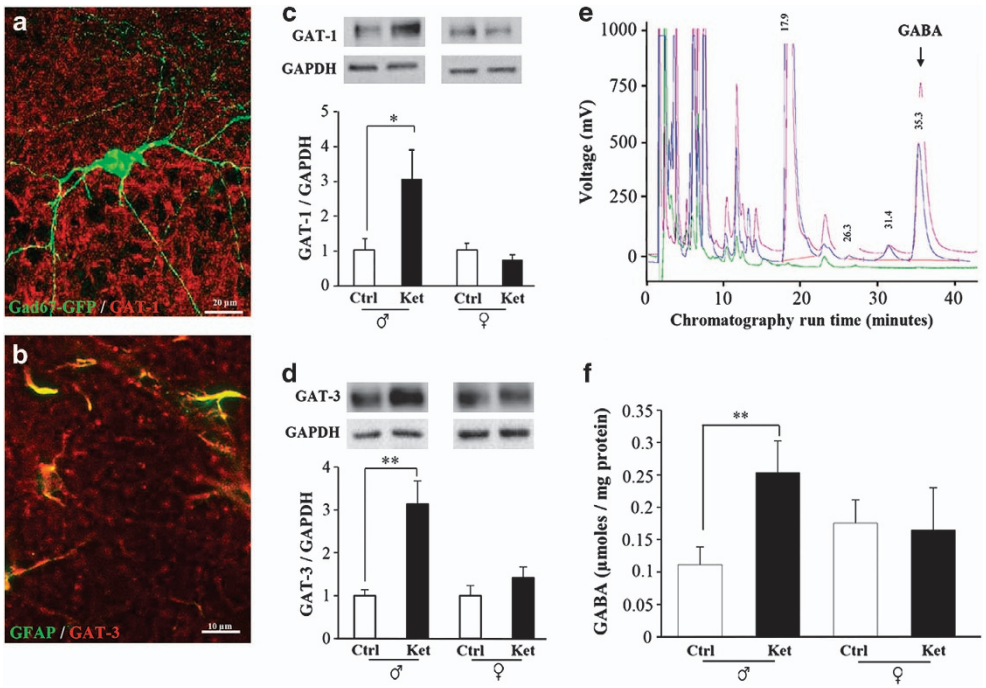

Figure 5 Long-term effect of *in vivo* prenatal exposure to ketamine on the expression levels of GABA transporters and GABA in the cortex of Gad67-GFP mice. (**a**) Photomicrographs showing GAT-1 immunolabeling in the cortex of P45 mice. GAT-1 puncta are widely distributed in the cortex, including on Gad67-GFP neurons. (**b**) Photomicrographs showing GAT-3 and GFAP immunolabeling in the cortex of P45 mice. (**c**) Quantification by western blotting of the effect of prenatal exposure to ketamine on GAT-1 levels in the cortex of male and female P45 mice. (**d**) Quantification by western blotting of the effect of prenatal exposure to ketamine on GAT-3 levels in the cortex of male and female P45 mice. (**e**) Representative HPLC chromatograms obtained by the elution solvent alone (green trace), the GABA standard (pink trace) and a sample from a mouse cortex (blue trace). (**f**) Quantification of GABA content in the cortex of male and female P45 mice. For western blotting experiments, each value represents the mean (± S.E.M.) of at least four independent experiments. For the quantification of GABA concentrations, each value represents the mean (± S.E.M.) of six animals per group. $^{*}P<0.05$; $^{**}P<0.01$ for ketamine *versus* control groups, Mann–Whitney *U*-test

GABAergic system of Gad67-GFP adult mice. In order to determine whether these alterations were associated with behavioral defects, we investigated the spontaneous activity of mice placed in a new and dark environment. Both males and females from the control group showed considerable locomotor activity as assessed by the distance covered during the first hour of the experiment (Figures 8a and b). Progressively, the mice reduced their activity and the distance covered remained stable after 2 h of recording (Figures 8a and b). No differences were found between males and females from the control group. Similarly, no differences were found between males from the control and the ketamine groups (Figure 8a). In contrast, the locomotor activity of females from the ketamine group was significantly increased when compared with that of control females (treatment effect yes $P<0.0001$; time effect yes $P<0.0001$; Bonferroni post-test $^{*}P<0.05$, $^{**}P<0.01$, $^{***}P<0.001$, $^{****}P<0.0001$ *versus* control; Figures 8b and c).

Discussion

Using Gad67-GFP mice, the present study shows that prenatal exposure to ketamine during a time-window in which GABAergic precursors are still migrating and differentiating results in (i) strong apoptotic death in the GEs and along the migratory routes; (ii) long-term alterations in interneuron density, primary dendrite numbers and spine morphologies; (iii) a sex-dependent deregulation of GABA and GABA transporter concentrations; (iv) sex-dependent defects in response to glutamate-induced calcium mobilization; and (v) long-term sex-dependent behavioral impairments in locomotor activity.

Ketamine increases the apoptotic death of immature GABAergic neurons in the MGE and migratory routes. In contrast to glutamatergic cortical neurons that originate from progenitors located in the pallium, cortical interneurons are generated in the subpallium and migrate tangentially into the cerebral cortex.[19,20] In particular, migrating neurons arising from the MGE reach the developing neocortex following several routes through the intermediate and marginal zones.[18] As we observed in a previous study that an NMDA antagonist, MK801, induced the death of immature GABAergic interneurons,[7] we raised the hypothesis of a possible deleterious effect of ketamine on the GABAergic population. Indeed, ketamine is an NMDA antagonist used both as an anesthetic in neonatal pediatrics and as a drug of abuse by young adults.[12,21] Using cultures of the MGE or whole brain slices from E15 embryos, we found that ketamine increased BAX levels and caspase-3 cleavage and activity, as well as altering mitochondrial integrity (Table 1). These effects were mainly observed in the MGE and overlapped with the migratory routes of GABAergic interneurons arising from

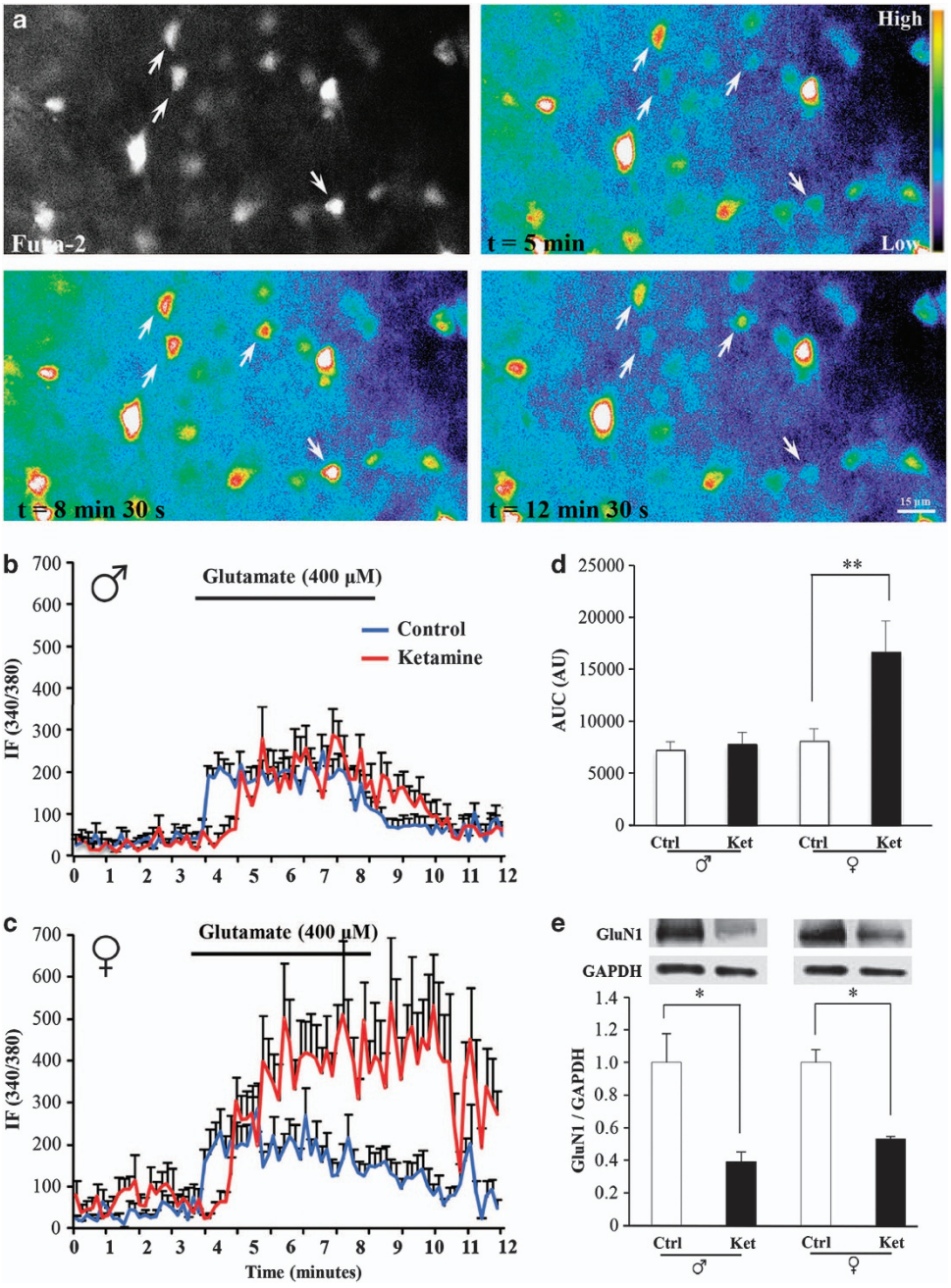

Figure 6 Long-term effect of *in vivo* prenatal exposure to ketamine on glutamate-induced intracellular calcium mobilization and GluN1 expression levels. (**a**) Photomicrographs showing Fura-2 loaded cells in the superficial layers of P15 brain slices (arrows) and false-color photomicrographs visualizing intracellular calcium variations after exposure to glutamate (400 μM). Mean recordings of the 340/380 ratio of the Fura-2 probe after exposure to glutamate (400 μM) in cortical slices from P15 males (**b**) and females (**c**) previously exposed *in utero* to ketamine (red lines) or from the control group (blue lines). (**d**) Quantification of the areas under the curves obtained by the measurement of intracellular calcium levels. (**e**) Quantification by western blotting of the effects of prenatal exposure to ketamine on GluN1 levels in the frontal cortex of male and female P15 mice. For calcimetry experiments, each value represents the mean (± S.E.M.) of 16 slices. *$P<0.05$; **$P<0.01$ for ketamine *versus* control groups, Mann–Whitney *U*-test

the MGE.[18] To reinforce these results, we took advantage of the characterization of specific transcription factor expression profiles throughout the migration and differentiation of cortical interneurons arising from the MGE.[20] Ketamine induced a significant decrease in the protein levels of Nkx2.1, DLX1 and LHX6 (Table 1), and immunohistochemistry showed that most of Nkx2.1-immunoreactive neurons entering the cortex were positive for cleaved caspase-3 after exposure to ketamine. Taken together, these data indicate that ketamine induces the apoptotic death of migrating GABAergic interneurons.

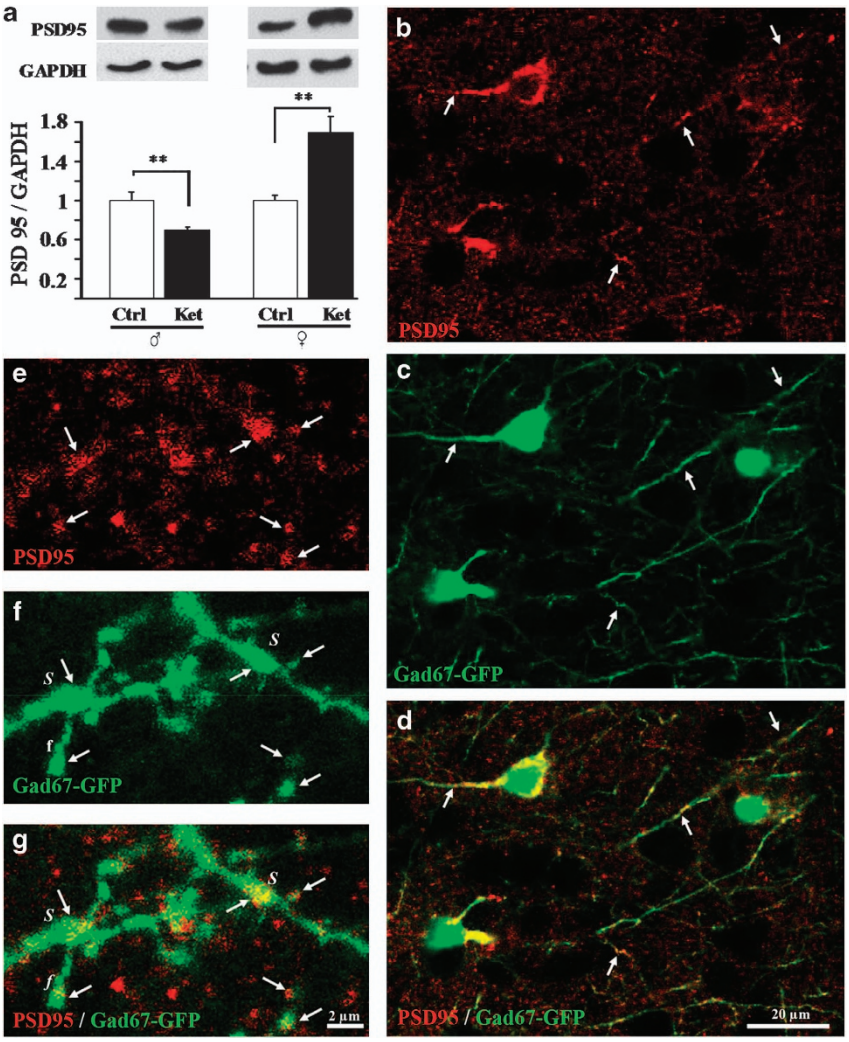

Figure 7 Immunohistochemical visualization of PSD95 expression in Gad67-GFP mice and quantification of the long-term effect of *in vivo* prenatal exposure to ketamine on PSD95 expression levels. (**a**) Quantification by western blotting of the effect of prenatal exposure to ketamine on PSD95 levels in the cortex of male and female Gad67-GFP mice at P15. (**b**–**d**) Low magnification photomicrographs visualizing PSD95 immunolabeling in the cortex of a Gad67-GFP mouse. Although PSD95 immunolabeling is not exclusively found in Gad67-GFP expressing neurons (**b**), numerous puncta co-localize with soma and dendrites (arrows) of the GABA interneurons (**c** and **d**). (**e**–**g**) High-magnification photomicrographs visualizing PSD95 immunolabeling and eGFP fluorescent dendrites. Note that several PSD95-immunoreactive puncta (**e**) co-localize with eGFP-positive dendrites (arrows) and are associated with different spine subtypes such as stubby (*S*) or filipodia (*f*) (**f** and **g**). For western blotting experiments, each value represents the mean (± S.E.M.) of at least four independent experiments. $^{**}P < 0.01$ for ketamine *versus* control groups, Mann–Whitney *U*-test

***In utero* exposure to ketamine alters the morphometric characteristics of mature Gad67-GFP interneurons in adult mice.** As *ex vivo* experiments support the view that ketamine specifically interacts with GABAergic interneurons arising from the MGE at E15, we investigated whether *in utero* exposure to ketamine could durably have an impact on the integration of GABA interneurons into the cortex. Morphometric analyses revealed a significant long-term reduction in GABAergic neuronal density in both male and female Gad67-GFP mice at P45. However, these effects were laminar dependent. Although in superficial layers (II–IV), the density of GFP- and GABA-positive neurons was decreased, in deep layers (V–VI) no difference of GABA density was found between control and ketamine groups. Altogether, these results suggest that ketamine exposure differently had an impact on the GABA interneurons, which colonized the superficial and the deep cortical layers. Interestingly, a recent report revealed that different lineages of GABA progenitors give rise to interneurons populating infra- and supra-granular cortical layers.[22] In particular, the authors showed that early-born interneurons preferentially populated deep layers V–VI, while late-born GABAergic neurons colonized layers II–IV.[22] Taken together, these data suggest a time- or lineage-specific sensitivity of GABA interneurons to ketamine.

3D reconstruction studies indicated that the number of primary neuritis, as well as spine density and subtypes were altered by ketamine in both sexes (Table 2). Although dendritic spines are typically associated with excitatory neurons,[23] a recent report using Gad65-GFP mice has shown that some types of GABAergic interneurons in the hippocampus also display a substantial number of spines.[24]

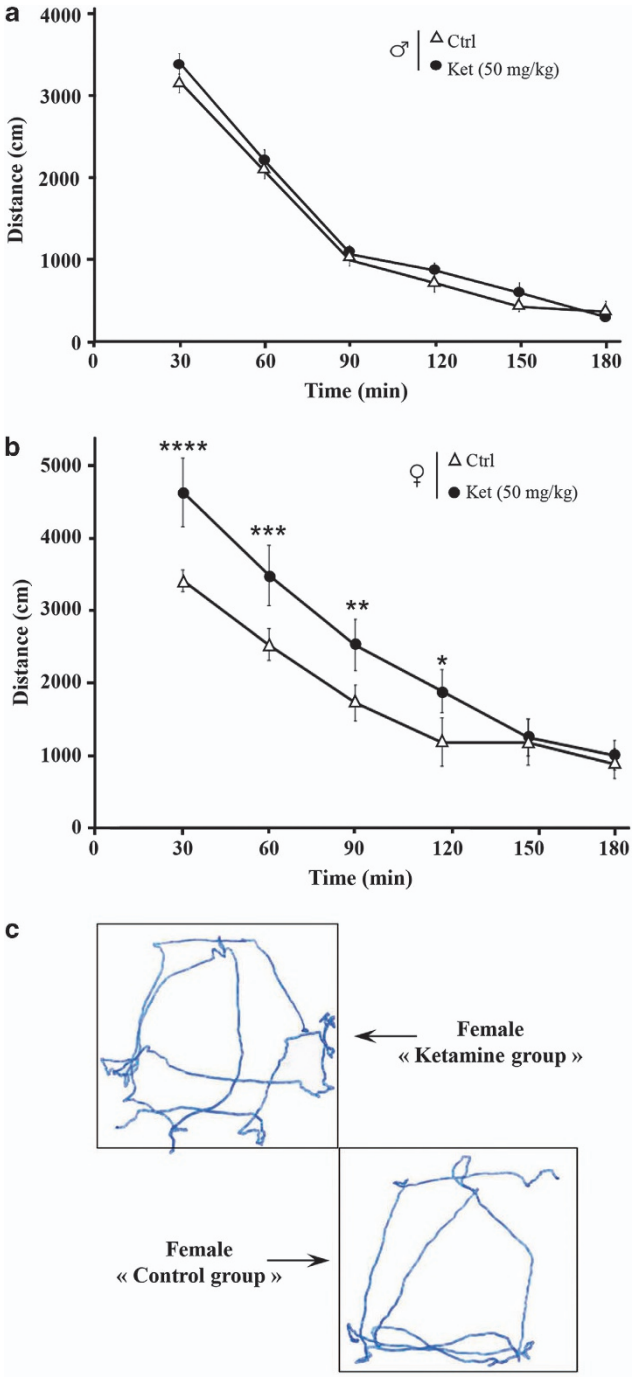

Figure 8 Long-term effect of *in vivo* prenatal exposure to ketamine on spontaneous horizontal locomotor activity in male and female P45 mice. Quantification over 3 h of the total distance covered every 30 min by P45 Gad67-GFP males (**a**) and females (**b**). Animals were exposed (Δ) or not (•) to ketamine *in utero*. (**c**) Visualization of the distance covered by female Gad67-GFP mice from the control and ketamine groups. Each value represents the mean (± S.E.M.) of 15 animals per group. $^{*}P<0.05$; $^{**}P<0.01$; $^{***}P<0.001$; $^{****}P<0.0001$ for ketamine *versus* control groups, Mann–Whitney *U*-test

In agreement with these results, our data reveal the presence of GABAergic spiny neurons in layers II–IV of the neocortex. Changes in dendritic arborization as well as spine density/morphology can be correlated with neuronal immaturity and/or differentiation impairments.[25–27] For example, filopodia are often considered immature spines and become less numerous with age.[27] Moreover, a recent *in vitro* study showed that calcium influx via NMDA receptor promoted spine maturation, while addition of the NMDA antagonist AP5 to the culture medium prevented morphological change from dendritic filopodia to dendritic spines.[28] Finally, we also found that PSD95 levels were downregulated in males, while they were upregulated in females. As (i) PSD95 is involved in the clustering of NMDARs at the synapses,[29] and (ii) during development, the expression of PSD95 at the post-synaptic density increases with maturation,[30] our data suggest that prenatal exposure to ketamine had a long-term impact on both the survival and differentiation of GABAergic interneurons, and influenced synaptic plasticity in a sex-specific manner.

***In utero* exposure to ketamine induces sex-dependent alterations of the neurochemical characteristics of the GABAergic system and long-term functional impairments.** The present study showed that *in utero* ketamine exposure induced long-term and sex-dependent alterations of the GABAergic system. In particular, GABA, GAT-1 and GAT-3 levels were significantly increased in males even 45 days after birth (Table 2), suggesting that despite a loss of GABAergic neurons in both sexes, the GABAergic neurotransmission was optimized in males. Consistent with this hypothesis a study from Tan *et al.*[31] showed that chronic ketamine exposure was able to upregulate the expression of the $GABA_A$ receptor in males. In addition, these gender differences were associated with exacerbated glutamate-induced calcium mobilization and higher motor activity only in females from the ketamine group (Table 2). Several data from the literature could be advanced to interpret this long-term sex-dependent differences. Indeed, a sexual differentiation of the brain during perinatal life has been previously described.[32,33] In particular, a critical period has been identified in rodents from late embryonic life to the first postnatal week.[34] During this period, (i) the GABAergic system is differentially regulated between males and females (for example, GABA and glutamic acid decarboxylase (GAD) expression levels are higher in males than in females at birth)[35] and (ii) a naturally occurring maturation process of the GABAergic system takes place in the neocortex.[36] Taken together, these results suggest that the compensatory processes that occurred in males and females following *in utero* ketamine exposure are different. At a physiological level, these differences can be explained by the different gonadal hormone environment between the sexes.[37] Indeed, several studies reported that gonadal hormones exert permanent organizational effects on the developing brain and thereby may induce long-term sex-specific behaviors.[37,38] Furthermore, factors such as estradiol have been shown to have an impact on the GABAergic transmission.[34] Consistent with these data from the literature, it has also been suggested that sex-specific sensitivity of the GABAergic system during perinatal life could underlie a sex-dependent susceptibility to certain diseases later on.[39]

Together, these results suggest that molecular and cellular defects following *in utero* ketamine exposure are associated with long-term functional impairments. They also raise the

Table 1 Summary of the short-term effects of ketamine on the MGE and immature cortex of Gad67-GFP mice on embryonic day 15 *ex vivo*

Gad67-GFP mice	Caspase-3 cleavage	Caspase-3 activity	BAX expression	Mitochondrial integrity	Nkx2.1, DLX1 and LHX6 levels	Nkx2.1 and caspase-3 co-localization
Females and males	↗	↗	↗	↘	↘	↗

Abbreviation: MGE, median ganglionic eminence; ↘, significantly decreased; ↗, significantly increased

Table 2 Summary of the long-term effects of prenatal ketamine exposure on morphological, molecular, functional and behavioral parameters in female and male Gad67-GFP mice *in vivo*

Gad67-GFP mice	Density of Gad67-GFP neurons	Number of primary dendrites	Density of dendritic spines	Cortical GABA levels	Expression of GAT1 and GAT3	Expression of Gad
Females	↘	↘	↘	≈	≈	↘
Males	↘	↘	↘	↗	↗	↘

Gad67-GFP mice	Expression of GluN1	Cortical glutamate levels	Expression of PSD95	Mobilization of calcium levels after glutamate stimulation	Spontaneous locomotor activity
Females	↘	≈	↗	↗	↗
Males	↘	≈	↘	≈	≈

≈, not significantly different from control mice; ↘, significantly decreased; ↗, significantly increased

question of the sex-related outcome of perinatal ketamine exposure in adulthood, which is already suspected for other factors such as bisphenol A, a chemical used in manufacturing plastics that has been shown to impair the GABAergic system in a sex-specific manner, inducing increased GABAergic activity in females throughout life.[40,41]

Does ketamine exposure present a risk during human brain development? In pediatrics, ketamine is used as an anesthetic during surgery and also as an analgesic to reduce pain in newborns, including preterm infants.[21,42] Based on the present results, in light of the potential for ketamine-induced neurodevelopmental impairments of the GABAergic system in humans, these clinical practices would be reconsidered. Indeed, even if ketamine exposure is limited in terms of duration, in preterm neonates the migration and differentiation of GABAergic interneurons is not yet complete.[17] Even more worrying is the fact that although ketamine (Special K) is routinely used as a drug of abuse[15] and shown to lead to severe damage (e.g., the atrophy of the frontal, parietal and occipital cortices) in the brains of adult consumers with chronic use,[43,44] its impact on the fetuses of ketamine-consuming pregnant women has not yet been considered.

In conclusion, using the Gad67-GFP mouse model, we show that ketamine exposure during development affects the survival and differentiation of GABAergic interneurons by triggering apoptosis in migrating neurons arising from the MGE, and by affecting their integration into the mature cortex over the long term. These molecular, morphological and functional alterations are associated with long-term sex-specific behavioral deficits. The present data raise the possibility that the use of ketamine in humans could be deleterious to the fetuses of addicted pregnant women and preterm neonates.

Materials and Methods

Animals. FVB-Tg(GadGFP)45704Swn transgenic mice (003718) were obtained from The Jackson Laboratory (Bar Harbor, ME, USA) and kept in a temperature-controlled room (21 ± 1 °C) with a 12 h/12 h light/dark cycle (lights on from 0700 to 1900 h) and free access to food and tap water. In these transgenic mice developed by Oliva *et al*.,[45] GABAergic interneurons arising from the GEs express enhanced green fluorescent protein under the control of the mouse Gad1 gene promoter. Animal care and experimentation complied with French and European guidelines for the care and use of laboratory animals (Council Directive 86/609/EEC, license number 21CAE035) and were carried out under the supervision of authorized investigators (B.J.G., authorization number7687 from the Ministère de l'Agriculture et de la Pêche).

Chemicals. Ketamine (Ketalar) was obtained from Parke-Davis (Berlin, Germany). NMDA was purchased from Tocris (Bristol, UK). The ratiometric intracellular calcium probe Fura-2 and the pluronic F-127 were from Invitrogen (Cergy Pontoise, France). Cresyl violet (acetate) and Hoechst 33258 were obtained from Sigma-Aldrich (Saint-Quentin Fallavier, France). Dulbecco's modified Eagle medium and the nutrient mixture F-12 (DMEM/F12) were from Life Technology (Saint Aubin, France). The Apo-ONE homogeneous caspase-3/7 kit was obtained from (Promega, Fitchburg, WI, USA). The glutamate assay kit was provided by BioVision (Milpitas, CA, USA). Alexa Fluor 488 donkey anti-rabbit IgG (A-21206) and Alexa Fluor 594 donkey anti-rabbit IgG (A-21207) were from Invitrogen. Goat polyclonal antibodies against GFAP (sc6170) and GluN1 (sc1467) and the rabbit polyclonal antibody against BAX (sc493) were from Santa Cruz Biotechnology (Santa Cruz, CA, USA). Rabbit monoclonal antibodies against synaptophysin (ab52636), PSD95 (ab76115) and Nkx 2.1 (ab76013), the goat polyclonal antibody against GFP (ab6673), the rabbit polyclonal antibodies against Dlx1 (ab111202), GAD65/67 (ab49832), GAT-1 (ab426), GAT-3 (ab431), Lhx6 (ab45983) and finally the mouse monoclonal GAPDH (ab8245) were from Abcam (Cambridge, UK). The antibody against GABA (A2052) was from Sigma-Aldrich. The rabbit polyclonal antibody against cleaved caspase-3 (9661) was purchased from Cell Signaling Technology (Boston, MA, USA). The JC-1 mitochondrial probe was purchased from Molecular Probes (Leiden, The Netherlands). The ECL RPN 2108 kit for western blotting was from Amersham (Orsay, France).

Preparation and treatment of E15 GE slices. Brain cortex slices were obtained from E15 mice. Although early tangential migration from the MGE begins around E11.5 in the mouse, slices prepared from E15 embryos contain, in addition to proliferating precursors, a large number of migrating cells in the developing

cortex.[46,47] In practice, pregnant mice at GD15 were killed by cervical dislocation. The fetuses were rapidly removed and placed in DMEM/F12 at 4 °C. The fetuses were killed by decapitation and their brains rapidly dissected in order to isolate the hemispheres. The overlying meninges were carefully removed and the neocortex immediately placed in ice-cold artificial cerebrospinal fluid (aCSF) containing (in mM): NaCl, 125; KCl, 3; $CaCl_2$, 2; NaH_2PO_4, 1.2; $MgSO_4$, 1.2; $NaHCO_3$, 26; D-glucose, 10; pH 7.4. Transverse slices (250 μM) were cut at 4 °C on a VT1000S Leica vibratome (Reuil-Malmaison, France), transferred to 24-well Costar plates (Cambridge, MA, USA) containing aCSF, and incubated for a 30-min recovery period at 37 °C in a humidified incubator under a controlled atmosphere of 5% CO_2/95% air. Next, slices were washed with fresh aCSF and treated for 12 or 24 h with 100 μM ketamine at 37 °C.

Determination of sex in embryos. For experiments performed on E15 GE slices, a control experiment was done to determine whether the effects of ketamine on apoptosis differed between females and males (Supplementary Figure 1). Embryos were sexed by amniotic cell staining.[48] Briefly, the amnion was isolated from the extra-embryonic membranes and fixed for 1 min in 3:1 methanol:glacial acetic acid in a Petri dish. Cells were stained for 5 min in 1% aqueous toluidine blue. After a 2-min wash in water, the membrane was crushed between a slide and a coverslip before microscopic observation. Unlike in males, amniotic cells from female embryos are characterized by a dense chromatin body at the periphery of the nucleus, which is clearly distinguishable from the paler, centrally located nucleoli (Supplementary Figure 1).

Measurement of caspase-3 activity. For caspase-3 activity measurements, GEs from E15 brain slices were microdissected, homogenized in 500 μl of hypotonic lysis buffer and 20 μg of proteins were incubated at 30 °C with 100 μl of caspase-3 buffer containing 1 μl of the caspase-3 substrate Z-DEVD-R110 provided with the Apo-ONE homogeneous caspase-3/7 kit (Promega). For each condition, the ipsilateral GE of the slice was used as control. Fluorescence intensity was quantified every 5 min for 2 h at excitation and emission wavelengths of 485 and 520 nm, respectively, using a Chameleon plate reader (Mustionkatu, Turku, Finland).

Measurements of mitochondrial integrity. Mitochondrial membrane potential was observed using the ratiometric probe JC-1. In healthy cells, the intact membrane potential allows the lipophilic dye JC-1 to enter the mitochondria where it accumulates and aggregates, producing an intense orange signal. In cells where the mitochondrial membrane potential has collapsed, the JC-1 probe remains unaggregated in the cytosol, where it is labeled green.[49] Acute E15 GE slices were treated for 10 h at 37 °C in the absence or presence of 100 μM ketamine, incubated for 30 min with 3 μl/ml JC-1 and finally washed twice for 5 min with phosphate buffer saline (PBS) at the same temperature. Fluorescence was visualized immediately without prior fixation at 485 and 530 nm excitation and emission wavelengths for green and 550 and 590 nm excitation and emission wavelengths for orange fluorescence, respectively. Green and orange signals were acquired and saved in TIFF format using a computer-assisted image analysis station (Metamorph, Roper Scientific, Evry, France).

***In vivo* exposure of Gad67-GFP mice to ketamine.** Ketamine (50 mg/kg) was administered daily by subcutaneous injection to pregnant FVB-Tg(GadGFP)45704Swn transgenic mice from GD15 to birth. Ketamine treatment was carried out at the same hour (1000 h) every day and the dose of ketamine chosen to induce analgesia for 3 h. The dose administered was based on previous comparative studies: in human, doses of ketamine recommended for sedation-analgesia ranged from 2 to 4 mg/kg i.m. and for anesthesia from 4 to 10 mg/kg i.m.[50] In mice, the dose of ketamine required to induce sedation is 80 mg/kg i.m.[51] A previous study from Young and co-workers[52] mentioned that in mice, doses of ketamine to induce analgesia/anesthesia are 8 to 16 times higher than those required for human and that such differences to induce a similar effect result, almost in part, from species characteristics in term of clearance properties. The control group was treated with 0.9% NaCl solution. No modification of the body weight of pregnant mice was seen between control and ketamine-treated groups, whereas the body weight of male and female pups from the ketamine group was significantly reduced ($P<0.05$; Supplementary Figure 4). After birth, pups were raised up to P45 to perform behavioral studies while the neurochemical and histological experiments were conducted in the sensorimotor cortex.

Immunohistochemistry. Brain slices from P45 animals were fixed overnight with 4% PFA in PBS and incubated overnight at 4 °C, with different primary antibodies diluted in incubation buffer (PBS containing 1% bovine serum albumin and 3% Triton X-100). Next, the slices were rinsed twice with PBS for 20 min and incubated in the same buffer containing the appropriate secondary antibody. Immunofluorescence images at low magnification were obtained by wide-field microscopy using a Leica DMI 6000B microscope and, afterwards, acquired images were deconvolved using the AutoQuant X_3 software (Media Cybernetics Inc., Rockville, MD, USA). For high-magnification images, acquisitions were done using a Leica TCS SP2 AOBS confocal laser scanning imaging system (Leica Microsystems AG, Nanterre, France). The specificity of the immunoreactions was verified by omitting the primary antibodies.

Quantification of Nkx2.1-positive cells immunoreactive for cleaved caspase-3. High-magnification images were acquired in the cortex of E15 brain slices by confocal microscopy and saved in a TIFF format. Images were subsequently opened in the Metamorph software and a grid was affixed on the image defining three regions of interest (ROIs). For each ROI, three parameters were quantified by using the 'count objects' application of the software, that is, the number of Hoechst-, cleaved caspase-3- and Nkx2.1-positive cells. Afterwards, results were expressed as 'Nkx2.1$^+$-cleaved caspase-3$^+$' co-labeled cells normalized to Hoechst$^+$ cells.

Western blot analysis. Cortices or GEs from control and ketamine-treated animals were homogenized in 300 μl of lysis buffer (50 μM Hepes; pH 7.5; 150 mM NaCl; 10 mM EDTA; 10 mM glycerophosphate; 100 mM sodium fluoride; 1% Triton X-100; 1 mM PMSF and PI cocktail). After centrifugation of the homogenate (20 000 $\times$ *g*, 15 min), the supernatants were used for western blotting. Fifty micrograms of protein extracts from cortical samples were suspended in Laemmli buffer (100 mM Hepes; pH 6.8; 10% β-mercaptoethanol; 20% SDS), boiled for 5 min and loaded onto a 10% SDS-polyacrylamide gel. After separation, proteins were electrically transferred onto a nitrocellulose membrane. The membrane was incubated with blocking solution (1 $\times$ TBS; 0.05% TWEEN 20; 5% non-fat milk) at room temperature for 1 h and incubated overnight with primary antibodies raised against BAX, cleaved caspase-3, DLX1, GAPDH, GluN1, GFP, GAT-1, GAT-3, LHX6, Nkx2.1, PSD95 and synaptophysin. After incubation with the corresponding secondary antibodies coupled to peroxidase (Santa Cruz Biotechnology), proteins were visualized using an enhanced chemiluminescence ECL Plus immunoblotting detection system (Amersham Biosciences Europe GmbH, Freiburg, Germany). The intensity of the immunoreactive bands was quantified using a blot analysis system (Bio-Rad Laboratories, Marne la coquette, France) and GAPDH was used as a loading control. Commercial markers (Seeblue pre-stained standard, Invitrogen) were used as molecular weight standards.

Measurement of intracellular calcium levels. Organotypic brain slices obtained from P15 mice were incubated for 15 min in aCSF containing 10 μM Fura-2 AM and 0.03% pluronic F-127. The slices were then washed twice for 5 min in aCSF at 37 °C and each slice was transferred to a 35-mm dish containing 1 ml of aCSF and immobilized using a nylon mesh. The temperature of the aCSF was kept constant at 37 °C and the slice was rinsed with aCSF. One volume of glutamate 400 μM was perfused into an equal volume of aCSF bathing the slice. The fluorescent signals associated with calcium-free and calcium-bound Fura-2 were measured by alternatively exciting the slices at 340 and 380 nm using a Leica DM fluorescent microscope equipped with a rapid shutter wheel. The emitted fluorescence was collected at 510 nm and the ratio of the two signals calculated using Metamorph software (Roper Scientific, Evry, France). Data were exported to the biostatistics software Prism (GraphPad Inc., San Diego, CA, USA), which was used to compute the maximal fluorescence intensity and the area under the curve.

Quantification of densities of Gad67-GFP cells and primary neuritis. For measurement of Gad67-GFP and GABAergic cell density, images were acquired and saved in TIFF format with a confocal laser scanning microscope (Noran Instruments, Middleton, WI, USA) using INTERVISION software (Noran Instruments). Images were subsequently opened in Mercator software and ROIs were drawn. Afterwards, a counting frame was defined within the ROI and a threshold was set in order to differentiate GFP-positive and GABA-positive cells from the background. By a segmentation process, the computer calculated the number and the cumulated area of objects within the ROI, yielding

cell number and cell density, respectively. For the measurement of Gad67-GFP-positive processes, a reference focal plane corresponding to the Gad67-GFP cell body was first defined. Next, *Z*-series of four images were acquired with a 2-μm step on both sides of the reference plane and saved in TIFF format. Afterwards, acquired images were deconvolved and compiled for 3D reconstruction using AutoQuant X_3 deconvolution software, for the quantification of the number of primary neurites per cell body.

Quantification of dendritic spine densities and morphology. The fine network of secondary and tertiary dendrites was acquired by confocal microscopy using a Leica DMI 6000B microscope and a Leica TCS SP2 AOBS confocal laser scanning imaging system (Leica Microsystems AG). *Z*-stack series of images were later deconvolved using AutoQuant X_3 deconvolution software and loaded into IMARIS imaging software (Bitplane, Zurich, Switzerland) for 3D reconstruction. The Filament Tracer function was used to assign and classify spines, yielding spine density and spine categories (stubby, filopodial or mushroom-shaped). Quantification was done on three slices per animals and three animals per group were analyzed. In particular, for a given slice, two ROIs were defined, two to three dendrites were quantified per ROI and the total number of quantified neuritis was fixed at 40 per group.

Determination of cortical GABA content. At P45, control and ketamine-exposed animals were killed by decapitation. The brains were quickly removed, the cortex were dissected on ice and homogenized by sonication at high frequency (70 Hz) for 4 s using a VibraCell Sonicator (Sonics and Materials, Newtwon, CT, USA) in ice-cold perchloric acid (0.1 mol/l) containing 1 g/l cysteine. Homogenates were centrifuged (10 000 $\times$ *g*, 10 min) and the supernatants filtered by pressure through 0.45-μm filters (Millipore, Courty Cork, Ireland) before GABA content determination. The pellets were resuspended in NaOH (0.1 M) and used for protein determination. Levels of GABA were determined by HPLC using a prior derivatization at 4 °C by adding 30 μl of sample to 10 μl of reactive solution prepared from o-phthaldialdehyde (40 mM) in 0.4 M borate buffer (pH 10.4) containing ethanol (100 g/l) and 2-mercaptoethanol (4 g/l). The 3-mn derivatization was followed by separation and detection using an HPLC system with electrochemical detection. A C18 reversed-phase column (3.0 $\times$ 150 mm, 3 μm; Supelcosil, Sigma-Aldrich, Bellefonte, PA, USA) was coupled with an electrochemical detector (Decade II, Antec Leyden) with a glassy carbon electrode set at 0.6 V *versus* a Ag/AgCl reference electrode. The mobile phase consisted of Na_2HPO_4 (0.1 M), methanol (240 g/l) and Na_2EDTA (0.15 mM) (pH 5.5), filtered through 0.45-μm filters (Millipore) and delivered by a pump (Spectrasystem P1000XR, Thermo Fisher Scientific, San Jose, CA, USA) at a flow rate of 0.3 ml/min. Samples (20 μl) were then injected into the HPLC system by means of an automatic device (AS 300; Spectra Physics, Santa Clara, CA, USA). Chromatograms were recorded and integrated using PC integration Azur software (Datalys, Le Touvet, France).

Glutamate concentration assay. The glutamate concentrations from P45 cortex extracts were quantified following the instructions provided within the glutamate assay kit. In practice, several dilutions of cortex extracts from control and ketamine-exposed animals were incubated with 100 μl of assay buffer in a 96-well plate. Afterwards, 100 μl of reaction mix was added to each well and the plate was incubated for 30 min at 37 °C prior measurement. The glutamate enzyme mix provided in the kit recognizes glutamate as a specific substrate leading to colorimetric quantification at 450 nm using a Chameleon plate reader (Mustionkatu, Turku, Finland). After background correction, glutamate concentrations were calculated using the glutamate standard curve.

Measurement of locomotor activity. Locomotor activity was assessed using a Versamax 4.2 apparatus (Accuscan Instruments Inc., Columbus, OH, USA). Animals were isolated for 10 min in individual cages before being placed in individual 20 cm $\times$ 20 cm $\times$ 30 cm compartments to limit anxiety, in a dark, sound-attenuated and temperature-regulated (20 $\pm$ 1 °C) room.[53] This test takes advantage of a rodent's natural tendency to explore a new environment. The recording apparatus was connected to a computer to process the data. Horizontal locomotor activity (the number of infrared beams crossed) and vertical locomotor activity (the number of infrared beams broken up to a height of 9 cm) were measured during six consecutive 30-min periods. In addition, video tracking using ANY-maze software (Stoelting, Wood Dale, IL, USA) was also performed to illustrate quantitative data acquired with the actimeter.

Statistical analysis. Statistical tests were run using the biostatistics software Prism (GraphPad Inc.). To analyze the effects of ketamine on caspase-3 activity, statistical analyses were used to compare the ketamine-treated ipsilateral side *versus* the control contralateral side using the Wilcoxon signed-rank test. To analyze the effects of ketamine on mitochondrial integrity, cell density, primary neurite and spine numbers, Nkx2.1-cleaved caspase 3 co-labeled cells, GABA and glutamate concentrations, western blot data and calcimetry, statistical analyses were used to compare ketamine-treated *versus* control conditions using the Mann–Whitney *U*-test. Locomotor activity was analyzed by two-way ANOVA (time/treatment) followed by Bonferroni's post test. For the distribution of spine subtypes, a χ^2-test was used.

Conflict of Interest

The authors declare no conflict of interests.

Acknowledgements. This work was supported by the Normandy University, INSERM, the Conseil Régional de Haute-Normandie, the European funds FEDER and INTERREG, the LARC-Neuroscience network and the Regional Platform for Cell Imaging (PRIMACEN). CR is a recipient of a fellowship from the Région Haute-Normandie.

1. Volpe JJ. Brain injury in premature infants: a complex amalgam of destructive and developmental disturbances. *Lancet Neurol* 2009; **8**: 110–124.
2. Jégou S, El Ghazi F, de Lendeu PK, Marret S, Laudenbach V, Uguen A *et al.* Prenatal alcohol exposure affects vasculature development in the neonatal brain. *Ann Neurol* 2012; **72**: 952–960.
3. Degos V, Peineau S, Nijboer C, Kaindl AM, Sigaut S, Favrais G *et al.* G protein-coupled receptor kinase 2 and group I metabotropic glutamate receptors mediate inflammation-induced sensitization to excitotoxic neurodegeneration. *Ann Neurol* 2013; **73**: 667–678.
4. Manning SM, Talos DM, Zhou C, Selip DB, Park HK, Park CJ *et al.* NMDA receptor blockade with memantine attenuates white matter injury in a rat model of periventricular leukomalacia. *J Neurosci* 2008; **28**: 6670–6678.
5. Cho GS, Lee JC, Ju C, Kim C, Kim WK. N-Methyl-D-aspartate receptor antagonists memantine and MK-801 attenuate the cerebral infarct accelerated by intracorpus callosum injection of lipopolysaccharides. *Neurosci Lett* 2013; **538**: 9–14.
6. McDonald JW, Silverstein FS, Cardona D, Hudson C, Chen R, Johnston MV. Systemic administration of MK-801 protects against N-methyl-D-aspartate- and quisqualate-mediated neurotoxicity in perinatal rats. *Neuroscience* 1990; **36**: 589–599.
7. Desfeux A, El Ghazi F, Jégou S, Legros H, Marret S, Laudenbach V *et al.* Dual effect of glutamate on GABAergic interneuron survival during cerebral cortex development in mice neonates. *Cereb Cortex* 2010; **20**: 1092–1108.
8. Ikonomidou C, Stefovska V, Turski L. Neuronal death enhanced by N-methyl-D-aspartate antagonists. *Proc Natl Acad Sci USA* 2000; **97**: 12885–12890.
9. Toriumi K, Mouri A, Narusawa S, Aoyama Y, Ikawa N, Lu L *et al.* Prenatal NMDA receptor antagonism impaired proliferation of neuronal progenitor, leading to fewer glutamatergic neurons in the prefrontal cortex. *Neuropsychopharmacol* 2012; **37**: 1387–1396.
10. Bhutta AT. Ketamine: a controversial drug for neonates. *Semin Perinatol* 2007; **31**: 303–308.
11. Dong C, Anand KJ. Developmental neurotoxicity of ketamine in pediatric clinical use. *Toxicol Lett* 2013; **220**: 53–60.
12. Brambrink AM, Evers AS, Avidan MS, Farber NB, Smith DJ, Martin LD *et al.* Ketamine-induced neuroapoptosis in the fetal and neonatal rhesus macaque brain. *Anesthesiology* 2012; **116**: 372–384.
13. Turner CP, Gutierrez S, Liu C, Miller L, Chou J, Finucane B *et al.* Strategies to defeat ketamine-induced neonatal brain injury. *Neuroscience* 2012; **210**: 384–392.
14. Lönnqvist PA, Walker SM. Ketamine as an adjunct to caudal block in neonates and infants: is it time to re-evaluate? *Br J Anaesth* 2012; **109**: 138–140.
15. Corazza O, Assi S, Schifano F. From "Special K" to "Special M": the evolution of the recreational use of ketamine and methoxetamine. *CNS Neurosci Ther* 2013; **19**: 454–460.
16. Morgan CJ, Curran HV. Ketamine use: a review. *Addiction* 2012; **107**: 27–38.
17. Letinic K, Zoncu R, Rakic P. Origin of GABAergic neurons in the human neocortex. *Nature* 2002; **417**: 645–649.
18. Kriegstein AR, Noctor SC. Patterns of neuronal migration in the embryonic cortex. *Trends Neurosci* 2004; **27**: 392–399.
19. Marin O. Cellular and molecular mechanisms controlling the migration of neocortical interneurons. *Eur J Neurosci* 2013; **38**: 2019–2029.
20. Wonders CP, Anderson SA. The origin and specification of cortical interneurons. *Nat Rev Neurosci* 2006; **7**: 687–696.
21. Saarenmaa E, Neuvonen PJ, Huttunen P, Fellman V. Ketamine for procedural pain relief in newborn infants. *Arch Dis Child Fetal Neonatal Ed* 2001; **85**: 53–56.
22. Ciceri G, Dehorter N, Sols I, Huang ZJ, Maravall M, Marín O. Lineage-specific laminar organization of cortical GABAergic interneurons. *Nat Neurosci.* 2013; **16**: 1199–1210.

23. Kwon HB, Sabatini BL. Glutamate induces de novo growth of functional spines in developing cortex. *Nature* 2011; **474**: 100–104.
24. Scheuss V, Bonhoeffer T. Function of dendritic spines on hippocampal inhibitory neurons. *Cereb Cortex* 2013; e-pub ahead of print 3 July 2013; doi:10.1093/cercor/bht171.
25. Orner DA, Chen CC, Orner DE, Brumberg JC. Alterations of dendritic protrusions over the first postnatal year of a mouse: an analysis in layer VI of the barrel cortex. *Brain Struct Funct* 2013; e-pub ahead of print 19 June 2013.
26. Yang K, Cao F, Sheikh AM, Malik M, Wen G, Wei H *et al.* Up-regulation of Ras/Raf/ERK1/2 signaling impairs cultured neuronal cell migration, neurogenesis, synapse formation, and dendritic spine development. *Brain Struct Funct* 2013; **218**: 669–682.
27. Zuo Y, Lin A, Chang P, Gan WB. Development of long-term dendritic spine stability in diverse regions of cerebral cortex. *Neuron* 2005; **46**: 181–189.
28. Hu HT, Hsueh YP. Calcium influx and postsynaptic proteins coordinate the dendritic filopodium-spine transition. *Dev Neurobiol* 2014; e-pub ahead of print 18 April 2014; doi:10.1002/dneu.22181.
29. Zheng CY, Seabold GK, Horak M, Petralia RS. MAGUKs synaptic development, and synaptic plasticity. *Neuroscientist* 2011; **17**: 493–512.
30. Sans N, Petralia RS, Wang YX, Blahos J 2nd, Hell JW, Wenthold RJ. A developmental change in NMDA receptor-associated proteins at hippocampal synapses. *J Neurosci* 2000; **20**: 1260–1271.
31. Tan S, Rudd JA, Yew DT. Gene expression changes in GABA(A) receptors and cognition following chronic ketamine administration in mice. *PLoS One* 2011; **6**: e21328.
32. Krishnan S, Intlekofer KA, Aggison LK, Petersen SL. Central role of TRAF-interacting protein in a new model of brain sexual differentiation. *Proc Natl Acad Sci USA* 2009; **106**: 16692–16697.
33. McCarthy MM, Arnold AP. Reframing sexual differentiation of the brain. *Nat Neurosci* 2011; **14**: 677–683.
34. Calza A, Sogliano C, Santoru F, Marra C, Angioni MM, Mostallino MC *et al.* Neonatal exposure to estradiol in rats influences neuroactive steroid concentrations, GABAA receptor expression, and behavioral sensitivity to anxiolytic drugs. *J Neurochem* 2010; **113**: 1285–1295.
35. Davis AM, Ward SC, Selmanoff M, Herbison AE, McCarthy MM. Developmental sex differences in amino acid neurotransmitter levels in hypothalamic and limbic areas of rat brain. *Neuroscience* 1999; **90**: 1471–1482.
36. Southwell DG, Paredes MF, Galvao RP, Jones DL, Froemke RC, Sebe JY *et al.* Intrinsically determined cell death of developing cortical interneurons. *Nature* 2012; **491**: 109–113.
37. Lenz KM, Nugent BM, McCarthy MM. Sexual differentiation of the rodent brain: dogma and beyond. *Front Neurosci* 2012; **6**: 1–13.
38. Davis AM, Grattan DR, McCarthy MM. Decreasing GAD neonatally attenuates steroid-induced sexual differentiation of the rat brain. *Behav Neurosci* 2000; **114**: 923–933.
39. Briggs SW, Galanopoulou AS. Altered GABA signaling in early life epilepsies. *Neural Plast* 2011; **11**: 527605–527621.
40. Anderson OS, Peterson KE, Sanchez BN, Zhang Z, Mancuso P, Dolinoy DC. Perinatal bisphenol A exposure promotes hyperactivity, lean body composition, and hormonal responses across the murine life course. *FASEB J* 2013; **27**: 1784–1792.
41. Yeo M, Patisaul H, Liedtke W. Decoding the language of epigenetics during neural development is key for understanding development as well as developmental neurotoxicity. *Epigenetics* 2013; **8**: 1128–1132.
42. Barois J, Tourneux P. Ketamine and atropine decrease pain for preterm newborn tracheal intubation in the delivery room: an observational pilot study. *Acta Paediatr* 2013; **102**: 534–538.
43. Kocsis B, Brown RE, McCarley RW, Hajos M. Impact of ketamine on neuronal network dynamics: translational modeling of schizophrenia-relevant deficits. *CNS Neurosci Ther* 2013; **19**: 437–447.
44. Wang C, Zheng D, Xu J, Lam W, Yew DT. Brain damages in ketamine addicts as revealed by magnetic resonance imaging. *Front Neuroanat* 2013; **7**: 23–39.
45. Oliva AA Jr, Jiang M, Lam T, Smith KL, Swann JW. Novel hippocampal interneuronal subtypes identified using transgenic mice that express green fluorescent protein in GABAergic interneurons. *J Neurosci* 2000; **20**: 3354–3368.
46. Lavdas AA, Grigoriou M, Pachnis V, Parnavelas JG. The medial ganglionic eminence gives rise to a population of early neurons in the developing cerebral cortex. *J Neurosci* 1999; **19**: 7881–7888.
47. Marín O, Rubenstein JL. A long, remarkable journey: tangential migration in the telencephalon. *Nat Rev Neurosci* 2001; **2**: 780–790.
48. Jiménez R, Barrionuevo FJ, Burgos M. A faster procedure for preparing amniotic cells for sexing embryos. *Technical Tips Online* 2001; **6**: 39–40.
49. Smiley ST, Reers M, Mottola-Hartshorn C, Lin M, Chen A, Smith TW *et al.* Intracellular heterogeneity in mitochondrial membrane potentials revealed by a J-aggregate-forming lipophilic cation JC-1. *Proc Natl Acad Sci USA* 1991; **88**: 3671–3675.
50. Pai A, Heining M. Ketamine. *Contin Educ Anaesth Crit Care Pain* 2007; **7**: 59–63.
51. Green CJ, Knight J, Precious S, Simpkin S. Ketamine alone and combined with diazepam or xylazine in laboratory animals: a 10 year experience. *Lab Anim* 1981; **15**: 163–170.
52. Young C, Jevtovic-Todorovic V, Qin YQ, Tenkova T, Wang H, Labruyere J *et al.* Potential of ketamine and midazolam, individually or in combination, to induce apoptotic neurodegeneration in the infant mouse brain. *Br J Pharmacol* 2005; **146**: 189–197.
53. Hart PC, Bergner CL, Smolinsky AN, Dufour BD, Egan RJ, Laporte JL *et al.* Experimental models of anxiety for drug discovery and brain research. *Methods Mol Biol* 2010; **602**: 299–321.

Supplementary Information accompanies this paper on Cell Death and Disease website (http://www.nature.com/cddis)